Letter

Testing the Stokes-Einstein relation with the hard-sphere fluid model

Hanqing Zhao[1,2,*] and Hong Zhao[1,3,†]

[1]*Department of Physics, Xiamen University, Xiamen 361005, Fujian, China*

[2]*Department of Modern Physics, University of Science and Technology of China, Hefei 230026, China*

[3]*Lanzhou Center for Theoretical Physics, Lanzhou University, Lanzhou, Gansu 730000, China*

(Received 24 June 2020; accepted 19 February 2021; published 9 March 2021)

The Stokes-Einstein (SE) relation has been widely applied to quantitatively describe the Brownian motion. Notwithstanding, here we show that even for a simple fluid, the SE relation may fail over a wide range of the Brownian particle's size. Namely, although the SE relation could be a good approximation for a large enough Brownian particle, a significant error may appear when decreasing the Brownian particle's size down to several hundred times the size of the fluid molecules, and the error increases with the decrease of the Brownian particle's size. The cause is rooted in the fact that the kinetic contribution to the diffusion coefficient is inversely proportional to the squared radius of the Brownian particle. After excluding the kinetic contribution, we show that the applicable range of the SE relation is expanded significantly.

DOI: 10.1103/PhysRevE.103.L030103

The Stokes-Einstein (SE) relation

$$DR = \frac{k_B T}{c\eta} \tag{1}$$

establishes a connection between the diffusion coefficient D of a Brownian particle and the shear viscosity η of the fluid it is immersed in. Here R is the radius of the Brownian particle, k_B is the Boltzmann constant, T is the fluid temperature, and c is a constant depending on the boundary conditions. It makes the Einstein relation [1] $\langle r(t)^2\rangle = 2Dt$ a quantitative law. Although the SE relation has been found invalid in certain extreme situations, such as in supercooled liquids [2,3], in glass-forming liquids [4–7], in dense complex medias [8–12], and in low-density gas [13,14], it is usually acknowledged for a simple fluid [15–26]. Consequently, this law is routinely used to compute D via the measurement of η, or to estimate the radius of molecules with measured D and η.

However, the test of the SE relation even in simple fluids is still insufficient. Previous verifications, experimental [2–5,7,18–20] or numerical [20–26], have focused on the special case where a tagged fluid molecule is adopted as the Brownian particle. Moreover, what these studies have checked is only the linear relationship between D and T of the SE relation with a fixed R. Whether and under what conditions DR is independent of the size R and mass M of the Brownian particle for a given fluid have not been systematically tested. Note that the size and mass dependence are of importance for applications, since in practice the radius of a Brownian particle can range from nanometer to millimeter [27,28] and the mass may vary in a wide range as well.

In this paper we test the size and mass dependence of the SE relation in the hard-sphere fluid model by large-scale numerical simulations. Earlier studies have made it clear that the diffusion of a particle is governed by both kinetics and hydrodynamics [29–35], and thus D involves a kinetic contribution and a hydrodynamic contribution, denoted by D_K and D_H, respectively. The former characterizes the momentum loss process due to random collisions between the Brownian particle and surrounding fluid molecules, while the latter is induced by the feedback momentum from surrounding fluid molecules. Our key progress is to work out a way to decompose D_K and D_H. By the decomposition we find that $D_K \sim R^{-2}$ in the entire fluid density regime. This scaling behavior indicates that the product DR should be R dependent when D_K cannot be neglected, and provides us a basis to infer the applicable range of the SE relation. Meanwhile, we find that $D_H \sim R^{-1}$, implying that

$$D_H R = \frac{k_B T}{c\eta} \tag{2}$$

should be a more appropriate version of the SE relation. We show that this version has a much wider applicable range than Eq. (1).

In principle the SE relation is a hydrodynamics law, since it is obtained on the basis of the Stokes law. The fact that Eq. (2) is superior to Eq. (1) indicates that to apply hydrodynamic laws, it is necessary to exclude the kinetic component. Showing the necessity of the decomposition of D in applying particle diffusion laws is the key issue of this paper. Accordingly, laws established on the basis of the kinetic theory should be also applied after excluding the hydrodynamic component. To support this proposition, we examine the Chapman-Enskog kinetic theory of the diffusion coefficient for molecules [10,36] and the gas-kinetic theory of the diffusion coefficient for Brownian particles. We show that, only when the hydrodynamic component is excluded, these theories can be justified without ambiguity. Besides, the

*Present address: Department of Physics, University of Colorado Boulder, Boulder, Colorado 80309, USA.

†zhaoh@xmu.edu.cn

applicable range of Eq. (2) can be identified on the basis of the decomposition.

Model and algorithm. We employ the hard-sphere fluid model [29,30,36] to perform our tasks. It consists of a sphere Brownian particle of mass M and radius R, and N fluid molecules. Each molecule has a unit mass $m = 1$ and a sphere shape of radius b. The packing fraction of fluid is given by $\phi = (4/3)\pi b^3 n$, where the number density n of fluid molecules is fixed at $n = 10^{-3}$ in our study. Note that with $R = b$ and $M = m$, the Brownian particle reduces to a fluid molecule. Initially, all the entities are placed evenly in a cubic box of side length L with periodic boundary conditions, and assigned a random velocity sampled from the equilibrium velocity distributions corresponding to temperature $T = 1$ (k_B is set to be unity) with the restriction that the total momentum is zero. Next, the system is evolved for a sufficiently long time to ensure that it has fully relaxed to the equilibrium state, then the velocity autocorrelation function (VACF), defined as $C(t) = \langle \mathbf{v}(\mathbf{t}) \cdot \mathbf{v}(\mathbf{0}) \rangle / 3$, is calculated, where $\mathbf{v}(\mathbf{t})$ is the velocity of the Brownian particle at time t. The collision between any two constituent entities are completely elastic.

To evolve the system numerically, an event-driven molecular dynamics algorithm is adopted [29,30,37]. As it is challenging to compute the VACF of a Brownian particle, the maximum number of fluid molecules and the maximum radius of the Brownian particle are set to be $N = 27\,000 (L = 300)$ and $R \leqslant 25$, respectively. For more details about the model and the algorithm, please see the Supplemental Material (SM) [38].

The hard-sphere model has an essential advantage for our purposes here, i.e., the radius of the Brownian particle is definitely defined. As a result, once DR is shown to vary with radius R or mass M in a given fluid (thus η and T are fixed), the violation of the SE relation can be concluded. To this end, only the diffusion coefficient needs to be calculated. The viscosity η of the fluid is required only when we need to determine the exact value of c.

Decomposition of the diffusion coefficient. The diffusion coefficient can be calculated by the Green-Kubo formula based on the VACF:

$$D(t) = \int_0^t C(t')dt'. \tag{3}$$

Since it involves kinetic and hydrodynamic contributions, the VACF can be decomposed as $C(t) = C_K(t) + C_H(t)$. The kinetic approach to the VACF is pioneered by Einstein [1]. The key insight is that the decay of the VACF is induced by random collisions of the Brownian particle with surrounding fluid molecules, by which the Brownian particle loses its initial momentum exponentially. The collisions are considered to be uncorrelated, which leads to [36]

$$C_K(t) = C(0) \exp\left(-\frac{C(0)}{D_K} t\right), \tag{4}$$

where $C(0) = k_B T / M$.

It has been known since the 1960s that the VACF also includes a hydrodynamic contribution: The momentum transferred to the fluid will feedback to the Brownian particle through a velocity vortex field [29,30,32,34,35] or, equally, through ring collisions [31,33]. The feedbacked momentum gives rise to $C_H(t)$. This effect can also be approximately formulated by the extended Langevin equation by involving a memory factor in the collisions [39,40]. These studies have established that $C_H(t)$ has a power-law tail at the long-time limit [36], i.e.,

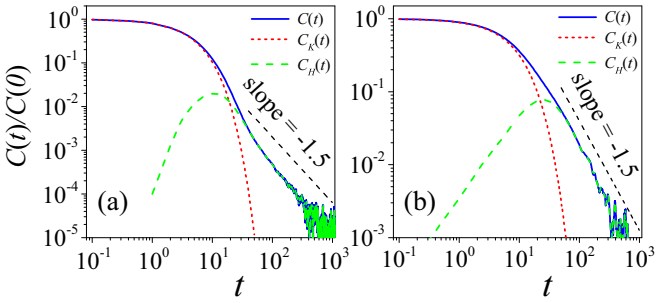

FIG. 1. The VACF of the Brownian particle in the fluid of $\phi = 0.11 (b = 3)$. (a) The Brownian particle is identical with the fluid molecules; $M = m$ and $R = b$; (b) $M = 24$ and $R = 20$.

$$C_H(t) \sim \frac{2k_B T}{3nm} [4\pi (D_K + \nu) t]^{-3/2}, \tag{5}$$

where $\nu = \eta/(mn)$ is the kinematic shear viscosity.

Our idea for separating $C_K(t)$ from $C(t)$ is as follows. In a short time, the momentum transferred from the Brownian particle to the fluid is little due to a few collisions; moreover, this part of transferred momentum does not contribute to the VACF of the Brownian particle, because a collision ring has not formed. A collision ring forms only when the momentum of the Brownian particle transferred to the fluid molecules comes back at a later moment to the Brownian particle itself through a collision chain of fluid molecules. Therefore, before the collision ring forms, $C(t)$ is identical to $C_K(t)$. In practice, we fit $C_K(t)$ by a proper D_K with Eq. (4) in a given short time interval $(0, t)$. The hydrodynamic effect is regarded to play no role if the fitting result does not change by decreasing t further.

Figures 1(a) and 1(b) show the VACF of the Brownian particle when it is identical with and different from the fluid molecules, respectively. With D_K determined by the best fitting introduced above, we obtain C_K and C_H ($C_H = C - C_K$) in the entire time window, shown in Fig. 1 as well. We see that the hydrodynamic effect of the Brownian particle is significantly larger when it has a bigger mass and a larger size than a fluid molecule. At large times, the VACFs converge to the long-time tail of $C(t) \sim t^{-3/2}$.

Testing kinetic theories of the diffusion coefficient. We first test the Chapman-Enskog kinetic theory for identical molecules, i.e., when the Brownian particle is a tagged fluid molecule with $R = b$ and $M = m$. In the first Sonine approximation [36], it gives $D_{\mathrm{CE}} = \frac{3}{8nb^2 g(\phi)} (\frac{k_B T}{m\pi})^{1/2}$ with $g(\phi) = (1 - \phi/2)/(1 - \phi)^3$. In Table I D_{CE} obtained with this formula for a different packing fraction is given, together with D_K of identical hard spheres calculated by the decomposition method. Surprisingly, D_K agrees with the theoretical prediction D_{CE} perfectly over the entire fluid regime. This fact indicates that, at least for the hard-sphere fluid, the Chapman-Enskog kinetic theory in the first Sonine approximation is accurate even in

TABLE I. Kinetic coefficients obtained by the Chapman-Enskog theory ($D_{\rm CE}$) and by the decomposition (D_K). The diffusion coefficient D is obtained by the Green-Kubo formula.

$b(\phi)$	1(0.004)	2(0.034)	3(0.11)	4(0.27)	4.5(0.39)	4.7(0.44)
$D_{\rm CE}$	52.3	12.1	4.35	1.50	0.763	0.552
D_K	52.3	12.2	4.35	1.49	0.760	0.550
D	53.5	12.6	4.93	2.06	1.04	0.519

the high-density regime. Particularly, the contribution of $g(\phi)$ from the first Sonine approximation is essential, and is also sufficient for this fluid model. In Table I we also provide D calculated by the Green-Kubo formula with the integral time being truncated at $t = 500$ (this truncation time is adopted throughout). (The possible correction induced by such a truncation will be discussed later.) We see that, although $D_{\rm CE}$ is very close to D in the low-density regime, the deviation may exceed 30% in the high-density regime, and there is no definite correlation between $D_{\rm CE}$ and D. Therefore, judging the prediction of $D_{\rm CE}$ by comparing it with D, as usually adopted in previous studies [23,26,30,41], is not appropriate for testing or applying such a law.

We then study the mass and size dependent behavior of D_k for a Brownian particle. In Fig. 2 we show D_K of the Brownian particle calculated by the decomposition method as a function of M with $R = 20$ [Fig. 2(a)] and as a function of R with $M = 24$ [Fig. 2(b)] for three packing fractions, $\phi = 0.034(b = 2)$, $0.11(b = 3)$, and $0.39(b = 4.5)$, respectively. Numerical errors, throughout this paper, are suppressed within the size of symbols by collecting a sufficient amount of ensemble samples. Note that usually $\phi = 0.3$ is considered as the boundary between gas and liquid phases [26]. Thus, our studies here cover both the gas and liquid regime. In Fig. 2(a) it shows that at a fixed R, D_K converges to a mass-independent constant as M increases, while in Fig. 2(b) it indicates that at a fixed large mass D_K decreases as

$$D_K \sim R^{-2} \tag{6}$$

when R is large.

For small Brownian particles in a low-density gas, the diffusion coefficient can be derived by the gas-kinetic theory [13,14]. It reads as $D_{\rm GK} = \frac{3}{8nR^2}(\frac{k_BT}{2m^*\pi})^{1/2}$ in the hard-sphere fluid model, where $m^* = mM/(M + m)$ is the reduced mass.

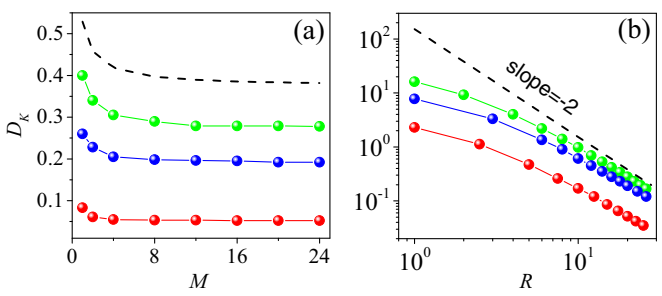

FIG. 2. D_K of the Brownian particle as a function of M at $R = 20$ (a) and of R at $M = 24$ (b). The dashed line is the prediction of the gas-kinetic theory. Three other curves (from top to bottom) are for $\phi = 0.034$, 0.11, and 0.39, respectively.

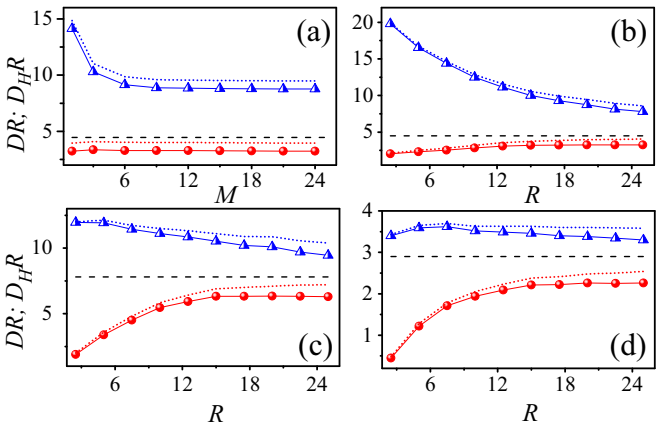

FIG. 3. Examination of the SE relation. DR (triangles) and D_HR (circles) of the Brownian particle as a function of M at $R = 20$ in the fluid of $\phi = 0.034$ (a), and of R at $M = 24$ in the fluids of $\phi = 0.034$ (b), $\phi = 0.11$ (c), and $\phi = 0.39$ (d), respectively. The dashed line in each panel indicates the predicated DR of $k_BT/c\eta$ with $c = 6\pi$. The dotted lines closing to the simulated results represent the estimated DR and D_HR in the thermodynamic limit, respectively.

It can be seen from Fig. 2 that, for characterizing the kinetic component D_K of D, this formula is actually qualitatively valid also for large Brownian particles over the entire fluid regime, not only limited for small Brownian particles in low-density gas. It is not quantitatively accurate out of the low-density limit regime since it is just a zero-order approximation corresponding to the Chapman-Enskog kinetic formula without the first Sonine correction [i.e., with $g(\phi) = 1$].

Testing the SE relation. Figure 3(a) reveals the M dependence of DR and D_HR in the fluid of $\phi = 0.034$. The size of the Brownian particle is fixed at $R = 20$. We see that DR varies at small masses but converges at large masses, while D_HR keeps mass independent. Therefore, light Brownian particles violate Eq. (1) but obey Eq. (2). Since D_H is mass independent, the mass-dependent behavior of DR should be ascribed to D_K.

Figure 3(b) shows the R dependence in the fluid of $\phi = 0.034$. The mass of the Brownian particle is fixed at $M = 24$. We see that DR decreases as R increases, while D_HR turns out to be approximately size independent for $R \geqslant 15$. Note that the converged value of D_HR in Fig. 3(b) is the same as that in Fig. 3(a). Therefore, D_HR becomes size insensitive for about $R > 15$. This fact also implies that $D_H \sim R^{-1}$ for large Brownian particles. Figures 3(c) and 3(d) show the R dependence in higher packing fractions. The mass of the Brownian particle is fixed also at $M = 24$. We see that they give the qualitatively similar results as in Fig. 3(b).

The R dependent behavior of D_K and D_H provides us a basis to estimate the applicable range of Eq. (1). As $DR \sim c_1/R + D_HR$, DR is expected to become approximately size independent at large enough R when $c_1/R \ll D_HR$ and as a result, $DR \sim D_HR$, where c_1 is a fitting parameter. This is a consequence of $D_K \sim R^{-2}$. As shown in Fig. 3, at $R = 15$, the deviation of DR from D_HR is about 300%, 170%, and 150% for the three packing fractions. The differences should disappear eventually with the increase of R. Fitting the data shown

in Fig. 2(b) we obtain $D_K \sim c_1 R^{-2}$ with $c_1 \approx 110$, 80, and 23 for the three packing fractions. Then we can infer that when R is larger than about $R \sim 2500$, 1500, and 1000, respectively, the deviation between DR and $D_H R$ will be smaller than 1%. As an estimation for real systems, we set the water molecule diameter (about 0.4 nm) to be the unit length in our model, the remarkable size-dependent effect may disappear for Brownian particles up to a micron in gas, and to hundreds of nanometers in liquid. Note that, though DR decreases continuously as R increases, the decreasing rate in liquid turns out to be much smaller than in gas, as c_1 is much smaller in liquid.

Corrections due to the finite-size effect and finite-time truncation. Due to the computation difficulty we have limited the system size at $N = 27\,000$ and truncated the upper limit of integral of Eq. (3) at $t = 500$ in calculating D and D_H. We consider the possible corrections induced by these treatments as follows. Within the time interval of $0 \leqslant t \leqslant 500$, we have checked that the VACF obtained with $N = 27\,000 (L = 300)$ overlaps with that obtained with $N = 125\,000 (L = 500)$ (see the SM [38]), indicating that $N = 27\,000$ is already large enough for calculating the VACF in this time interval. However, since the VACF has a long-time tail, the upper limit of integral may contribute a remarkable correction to D and D_H. As can be seen in Fig. 1, the power-law tail of $C(t) \sim t^{-3/2}$ has already been fixed before $t = 500$. Furthermore, it can be verified that at a fixed packing fraction, the VACFs with different M and R converge roughly to the same long-time tail. In the fluid of $\phi = 0.11$ for example, VACFs converge to the tail of $C(t) \sim 0.6t^{-3/2}$. Accordingly, the correction due to the finite-time truncation can be evaluated, i.e., $D_{\rm tr} = \int_{500}^{\infty} C(t)dt$. In this way we obtain the estimations of D and D_H in the thermodynamic limit. The dotted lines in Fig. 3 show the results of DR and $D_H R$ with the estimated corrections, respectively. Since both DR and $D_H R$ are equally lifted, the correction does not affect the estimation of the applicable range of Eq. (1). For more details please see the SM [38].

To judge whether DR and $D_H R$ can finally converge to $k_B T/c\eta$ we need to calculate the shear viscosity η, or equally the kinematic shear viscosity ν. Following the method in Refs. [23,42], we obtain $\nu = 11.8 \pm 0.1, 6.8 \pm 0.1$, and 18.3 ± 0.2 for the three packing fractions, respectively. In Fig. 3 the dashed lines represent $k_B T/c\eta$ with the sticking boundary condition, i.e., with $c = 6\pi$. We see that the estimated $D_H R$ of the infinite large system has approached the predictions of $c = 6\pi$ particularly in the low-density fluids. Nevertheless, since the finite-size effects have not been fully considered, such as the finite-size effect of ν, we have to leave it open whether DR and $D_H R$ can accurately converge to the prediction of $c = 6\pi$.

A phenomenological derivation of Eq. (2). Our reasoning is similar to that for the long-time tail in Ref. [36] (p. 246), but with the key difference that we take the delay effect into account. Suppose that at $t = 0$ the Brownian particle resides at $\mathbf{r} = 0$. Then its initial momentum gradually transfers to the surrounding fluid molecules by collisions, and spreads out by the viscosity and sound modes. The momentum density $\Psi(r, t)$ carried by the viscosity mode relaxes diffusively as $\Psi(r, t) \sim \exp[-r^2/(4\nu t)]$. This mode feeds the momentum back to the Brownian particle and contributes to the hydrodynamic component D_H. The characteristic radius of the pack region of $\Psi(r, t)$ expands as $r_c = \sqrt{4\nu t}$. Assuming the Brownian particle floats at the average velocity of fluid molecules in this region, one obtains $C_H(t) \sim [4\pi(D_K + \nu)t]^{-3/2}$. By considering more details, Eq. (5) is derived [36]. Based on this reasoning, we further emphasize that for a Brownian particle of radius R, the viscosity mode is physically meaningless for $t < R^2/4\nu$ since $r_c < R$ in this time period. In other words, the feedback begins to play a role only after $t = R^2/4\nu$. Then, plugging Eq. (5) into Eq. (3), the lower limit of integral should be larger than $t = R^2/4\nu$. With this consideration we obtain an estimation of D_H, i.e., $D_H \sim \int_{R^2/4\nu}^{\infty} C_H(t)dt \sim \frac{k_B T\sqrt{\nu}}{3\pi m R[\pi(D_K+\nu)]^{3/2}}$. This result gives, on one hand, $D_H R \sim k_B T/3\sqrt{\pi}\pi\eta$ for large Brownian particles when $D_K \ll \nu$, which is very close to Eq. (2) with $c = 6\pi$. On the other hand, it explains that Eq. (2) may also fail for small enough Brownian particles when D_K also contributes a R dependent component. This feature implies that a full exclusion of the kinetic effect fails. Nevertheless, the condition of $D_K \ll \nu$ for Eq. (2) can be easily satisfied than that of $D_K \ll D_H \sim 1/R\nu$ for Eq. (1). Extrapolating D_K based on the scaling law of $D_K \sim c_1 R^{-2}$, we get that $R > 32$, 34, and 35 can assure $D_K/\nu < 1\%$ for the three packing fractions, respectively. These results agree in order with the simulation results of Fig. 3, where the dependence of $D_H R$ on R becomes insensitive for $R \geqslant 15$. Therefore, Eq. (2) has a much broader applicable range than Eq. (1) has.

In summary, by decomposing the diffusion coefficient into the kinetic component and the hydrodynamic component, we reveal that the former scales as $D_K \sim R^{-2}$ and is mass dependent, while the latter scales as $D_H \sim R^{-1}$ and is mass independent. Therefore, Eq. (2) instead of Eq. (1) should be considered as a more appropriate version of the SE relation. Equation (1) is applicable for Brownian particles with sufficient large R and M when D_K is negligible with respect to D_H, which demands R should be several hundred times larger than the size of the fluid molecules and M should be tenfold larger than the mass of the fluid molecules at least. Equation (2) is found to fail also for small Brownian particles when their sizes are comparable with the fluid molecules. Theoretical analysis reveals that Eq. (2) is accurate under the condition of $D_K \ll \nu$, and fails when $D_K \approx \nu$, in which case D_H becomes coupled with D_K and thus a full decomposition of the hydrodynamic component fails. These results indicate that a formula that covers the spectrum of Brownian particles around the size of fluid molecules is still lacking.

The decomposition is also helpful for examining kinetic theories. The gas-kinetic theory predicts that the diffusion coefficient for small Brownian particles in low-density gas should be inversely proportional to the squared R. Our results show that such a scaling law indeed generally holds for Brownian particles in the entire fluid regime for the D_K decomposed from D. Meanwhile, the results also reveal that a quantitatively accurate formula of D_K is still a topic of future studies. In addition, when the Brownian particle is a tagged fluid molecule, judged by the D_K instead of D we verify that the Chapman-Enskog kinetic theory in the fist Sonine approximation is perfectly accurate in the entire fluid regime. Therefore, particle diffusion theories are usually established on either the kinetics or the hydrodynamics, and

thus they should be applied or tested on the basis of the decomposition.

We would like to point out that a fine experimental test of the size and mass dependence of the SE relation is becoming possible. Indeed, traditional experimental techniques [15–17,43–45] have already allowed one to measure the trajectory of a single Brownian particle of hundreds of nanometers. In recent years, thanks to the state-of-the-art experimental developments, the measurements of displacement as well as instant velocity of a single Brownian particle have been available [46–51], and thus make it possible to obtain an accurate $C(t)$ experimentally and to decompose D_K and D_H.

Acknowledgments. This work is supported by the NSFC (Grants No. 11335006, No. 11975189, and No. 12047501).

[1] A. Einstein, In the movement of small particles suspended in stationary liquids required by the molecular-kinetic theory of heat, Ann. Phys. **17**, 549 (1905).

[2] E. Rössler, Indications for a Change of Diffusion Mechanism in Supercooled Liquids, Phys. Rev. Lett. **65**, 1595 (1990).

[3] M. Dzugutov, S. I. Simdyankin, and F. H. M. Zetterling, Decoupling of Diffusion from Structural Relaxation and Spatial Heterogeneity in a Supercooled Simple Liquid, Phys. Rev. Lett. **89**, 195701 (2002).

[4] S. R. Becker, P. H. Poole, and F. W. Starr, Fractional Stokes-Einstein and Debye-Stokes-Einstein Relations in a Network-Forming Liquid, Phys. Rev. Lett. **97**, 055901 (2006).

[5] M. G. Mazza, N. Giovambattista, H. E. Stanley, and F. W. Starr, Connection of translational and rotational dynamical heterogeneities with the breakdown of the Stokes-Einstein and Stokes-Einstein-Debye relations in water, Phys. Rev. E **76**, 031203 (2007).

[6] L. Xu, F. Mallamace, Z. Yan, F. W. Starr, S. V. Buldyrev, and H. E. Stanley, Appearance of a fractional Stokes–Einstein relation in water and a structural interpretation of its onset, Nat. Phys. **5**, 565 (2009).

[7] A. Dehaoui, B. Issenmann, and F. Caupin, Viscosity of deeply supercooled water and its coupling to molecular diffusion, Proc. Natl. Acad. Sci. USA **112**, 12020 (2015).

[8] Y. Rosenfeld, A quasi-universal scaling law for atomic transport in simple fluids, J. Phys. Condens. Matter **11**, 5415 (1999).

[9] M. Dzugutov, Addendum: A universal scaling law for atomic diffusion in condensed matter, Nature (London) **411**, 720 (2001).

[10] J. L. Bretonnet, Self-diffusion coefficient of dense fluids from the pair correlation function, J. Chem. Phys. **117**, 9370 (2002).

[11] C. Kaur, U. Harbola, and S. P. Das, Nature of the entropy versus self-diffusivity plot for simple liquids, J. Chem. Phys. **123**, 034501 (2005).

[12] L. Ning, P. Liu, Y. Zong, R. Liu, M. Yang, and K. Chen, Universal Scaling Law for Colloidal Diffusion in Complex Media, Phys. Rev. Lett. **122**, 178002 (2019).

[13] P. S. Epstein, On the resistance experienced by spheres in their motion through gases, Phys. Rev. **23**, 710 (1924).

[14] Z. Li and H. Wang, Drag force, diffusion coefficient, and electric mobility of small particles. I. Theory applicable to the free-molecule regime, Phys. Rev. E **68**, 061206 (2003).

[15] T. G. Mason, K. Ganesan, J. H. Van Zanten, D. Wirtz, and S. C. Kuo, Particle Tracking Microrheology of Complex Fluids, Phys. Rev. Lett. **79**, 3282 (1997).

[16] S. Barhoum, S. Palit, and A. Yethiraj, Diffusion NMR studies of macromolecular complex formation, crowding and confinement in soft materials, Prog. Nucl. Magn. Reson. Spectrosc. **94**, 1 (2016).

[17] S. Palit, L. He, W. A. Hamilton, A. Yethiraj, and A. Yethiraj, Combining Diffusion NMR and Small-Angle Neutron Scattering Enables Precise Measurements of Polymer Chain Compression in a Crowded Environment, Phys. Rev. Lett. **118**, 097801 (2017).

[18] F. H. Stillinger and J. A. Hodgdon, Translation-rotation paradox for diffusion in fragile glass-forming liquids, Phys. Rev. E **50**, 2064 (1994).

[19] D. J. Wilbur, T. DeFries, and J. Jonas, Self-diffusion in compressed liquid heavy water, J. Chem. Phys. **65**, 1783 (1976).

[20] H. J. Parkhurst, Jr. and J. Jonas, Dense liquids. II. The effect of density and temperature on viscosity of tetramethylsilane and benzene, J. Chem. Phys. **63**, 2705 (1975).

[21] K. R. Harris, Scaling the transport properties of molecular and ionic liquids, J. Mol. Liq. **222**, 520 (2016).

[22] K. R. Harris, The fractional Stokes–Einstein equation: Application to Lennard-Jones, molecular, and ionic liquids, J. Chem. Phys. **131**, 054503 (2009).

[23] B. J. Alder, D. M. Gass, and T. E. Wainwright, Studies in molecular dynamics. VIII. The transport coefficients for a hard-sphere fluid, J. Chem. Phys. **53**, 3813 (1970).

[24] S. Tang, G. T. Evans, C. P. Mason, and M. P. Allen, Shear viscosity for fluids of hard ellipsoids: A kinetic theory and molecular dynamics study, J. Chem. Phys. **102**, 3794 (1995).

[25] B. Liu, J. Goree, and O. S. Vaulina, Test of the Stokes-Einstein Relation in a Two-Dimensional Yukawa Liquid, Phys. Rev. Lett. **96**, 015005 (2006).

[26] N. Ohtori, H. Uchiyama, and Y. Ishii, The Stokes-Einstein relation for simple fluids: From hard-sphere to Lennard-Jones via WCA potentials, J. Chem. Phys. **149**, 214501 (2018).

[27] R. A. M. Fouchier, S. Herfst, and A. D. M. E. Osterhaus, Restricted data on influenza H5N1 virus transmission, Science **335**, 662 (2012).

[28] D. Shindell and C. J. Smith, Climate and air-quality benefits of a realistic phase-out of fossil fuels, Nature (London) **573**, 408 (2019).

[29] B. J. Alder and T. E. Wainwright, Velocity Autocorrelations for Hard Spheres, Phys. Rev. Lett. **18**, 988 (1967).

[30] B. J. Alder and T. E. Wainwright, Decay of the velocity autocorrelation function, Phys. Rev. A **1**, 18 (1970).

[31] J. R. Dorfman and E. G. D. Cohen, Velocity Correlation Functions in Two and Three Dimensions, Phys. Rev. Lett. **25**, 1257 (1970).

[32] M. H. Ernst, E. H. Hauge, and J. M. J. Van Leeuwen, Asymptotic time behavior of correlation functions. I. Kinetic terms, Phys. Rev. A **4**, 2055 (1971).

[33] J. R. Dorfman and E. G. D. Cohen, Velocity-correlation functions in two and three dimensions: Low density, Phys. Rev. A **6**, 776 (1972).

[34] Y. Pomeau and P. Resibois, Time dependent correlation functions and mode-mode coupling theories, Phys. Rep. **19**, 63 (1975).

[35] M. H. Ernst, E. H. Hauge, and J. M. J. Van Leeuwen, Asymptotic time behavior of correlation functions. II. Kinetic and potential terms, J. Stat. Phys. **15**, 7 (1976).

[36] J. P. Hansen and I. R. McDonald, *Theory of Simple Liquids* (Academic, New York, 2006).

[37] M. Marín, Event-driven hard-particle molecular dynamics using bulk-synchronous parallelism, Comput. Phys. Commun. **102**, 81 (1997).

[38] See Supplemental Material at http://link.aps.org/supplemental/10.1103/PhysRevE.103.L030103 for the detailed description of the model, the algorithm, and the discussions of the finite-size effect.

[39] R. Zwanzig and M. Bixon, Hydrodynamic theory of the velocity correlation function, Phys. Rev. A **2**, 2005 (1970).

[40] W. B. Russel, Brownian motion of small particles suspended in liquids, Annu. Rev. Fluid Mech. **13**, 425 (1981).

[41] H. Sigurgeirsson and D. M. Heyes, Transport coefficients of hard sphere fluids, Mol. Phys. **101**, 469 (2003).

[42] R. García-Rojo, S. Luding, and J. J. Brey, Transport coefficients for dense hard-disk systems, Phys. Rev. E **74**, 061305 (2006).

[43] D. Dürr and H. Spohn, Brownian motion and microscopic chaos, Nature (London) **394**, 831 (1998).

[44] N. Y. C. Lin, M. Bierbaum, and I. Cohen, Determining Quiescent Colloidal Suspension Viscosities Using the Green-Kubo Relation and Image-Based Stress Measurements, Phys. Rev. Lett. **119**, 138001 (2017).

[45] H. Kim, K. Muller, O. Shardt, S. Afkhami, and H. A. Stone, Solutal Marangoni flows of miscible liquids drive transport without surface contamination, Nat. Phys. **13**, 1105 (2017).

[46] Y. Han, A. M. Alsayed, M. Nobili, J. Zhang, T. C. Lubensky, and A. G. Yodh, Brownian motion of an ellipsoid, Science **314**, 626 (2006).

[47] T. Li, S. Kheifets, D. Medellin, and M. G. Raizen, Measurement of the instantaneous velocity of a Brownian particle, Science **328**, 1673 (2010).

[48] T. Franosch, M. Grimm, M. Belushkin, F. M. Mor, G. Foffi, L. Forró, and S. Jeney, Resonances arising from hydrodynamic memory in Brownian motion, Nature (London) **478**, 85 (2011).

[49] S. Kheifets, A. Simha, K. Melin, T. Li, and M. G. Raizen, Observation of Brownian motion in liquids at short times: Instantaneous velocity and memory loss, Science **343**, 1493 (2014).

[50] I. A. Martínez, D. Petrosyan, A. Guéry-Odelin, E. Trizac, and S. Ciliberto, Engineered swift equilibration of a Brownian particle, Nat. Phys. **12**, 843 (2016).

[51] X. Fu, B. Chen, J. Tang, M. Th. Hassan, and A. H. Zewail, Imaging rotational dynamics of nanoparticles in liquid by 4D electron microscopy, Science **355**, 494 (2017).